Carbohydrate Polymers 78 (2009) 833–840

Contents lists available at ScienceDirect

Carbohydrate Polymers

journal homepage: www.elsevier.com/locate/carbpol

Synthesis, characterization and aqueous dispersion of dextran-g-poly(1,4-dioxan-2-one) copolymers

Madhab Prasad Bajgai [a], Daman Chandra Parajuli [a], Jung An Ko [a], Hyo Kyoung Kang [b], Myung-Seob Khil [b], Hak Yong Kim [b,*]

[a] Department of Bionanosystem Engineering, Chonbuk National University, Jeonju 561-756, Republic of Korea
[b] Department of Textile Engineering, Chonbuk National University, Jeonju 561-756, Republic of Korea

ARTICLE INFO

Article history:
Received 11 February 2009
Received in revised form 5 June 2009
Accepted 6 July 2009
Available online 12 July 2009

Keywords:
Biopolymers
Micelles
Graft copolymers
Dextran

ABSTRACT

A novel biodegradable graft copolymer, dextran-g-poly(1,4-dioxan-2-one) (PODEX), was synthesized through the ring-opening polymerization (ROP) of 1,4-dioxan-2-one (PDO) onto a dextran backbone. Initially, dextran was silylated with 1,1,1,3,3,3-hexamethyldisilazane. The grafting from pathway was conducted with various (30–70) PDO/OH feed ratios to obtain PODEX copolymers with a various PPDO graft structures. Graft copolymers were characterized by FT-IR, ^{1}H and ^{13}C NMR, DSC, TGA, and WAXD. Molecular weights of the PODEX copolymers (M_W: 94,700–117, 300 Da), glass transition temperature (−29 to −17 °C), melting temperature (82–100 °C), and crystallinity (32–40%) were increased with the content of PPDO. AFM observations revealed that polymeric micelles were spherical and uniform in morphology with around 30–58 nm diameter. Critical micelle concentration (CMC) of self-assembled system was significantly decreased from 3.2 to 1.09 mg/L with the increment of PPDO.

1. Introduction

Significant research is ongoing to the development of biodegradable polymers, initially with the purpose of designing resorbable biomaterials in surgery, drug delivery, and tissue-engineering applications (Ouchi, Kontani, & Ohya, 2003). The promising requirement for a polymer to be used in biomedical application is its biocompatibility in specific environments, together with the nontoxicity of the degraded products (Pachence & Kohn, 2000). Polysaccharides such as cellulose, starch, chitosan, and dextran are attractive biopolymers for biomedical and pharmacological research fields due to their biocompatibility, biodegradability, and cell surface recognition sites (Abdurrahmanoglu & Firat, 2007). Specifically, dextran, which consists mainly of α-1,6 linked anhydroglucose unit and partly of α-1,2-, α-1,3- or α-1,4-linked side chains, has been used as plasma volume expander for several years (Chen, Jo, & Park, 1995; Sabatie et al., 1988). However, polysaccharide-based biopolymers have limitations for their application due to poor-long term stability, weak mechanical properties, and difficulty in processibility (Choi, Kim, & Park, 1999). Hence, there is need of tailoring the natural biopolymers with synthetic moieties to improve the drawbacks as mentioned above.

On the other hand, aliphatic polyesters such as poly(ε-caprolactone) (PCL), poly(lactide) (PLA), poly(glycolide) (PGA), poly(*p*-dioxanone) (PPDO), poly(lactide-co-glycolide) (PLGA), and their copolymers are extensively used in medical applications (Anderson & Shie, 1997; KC, Aryal, Bhattarai, Khil, & Kim, 2007). Such biodegradable materials are important in biomedical fields owing to their superior mechanical properties, good biodegradability, and completely degradable materials without toxic by-products (Bhattarai et al., 2006; Kim, Khil, Kim, Lee, & Jahng, 2006; Nishida, Konno, Ikeda, & Tokiwa, 2000; Young, Min, Lee, Lee, & Park, 2005). Hence, these materials have been used in the tissue-engineering of cartilage, bone, tendon, skin, and liver and heart valves. Among above-mentioned aliphatic polyesters, poly(*p*-dioxanone) (PPDO) has its own special characteristics due to the presence of both ether and ester bonds in its structural unit (Sabatie et al., 1988). The ester bond accounts for the ultimate biodegradability, whereas the ether bond and an additional CH_2 in its molecular structure endow the hydrophilicity and flexibility to the molecule (Sabatie et al., 1988). Importantly, PPDO shows lower degradation via hydrolysis, due to the lower concentration of ester groups, as compared to PGA and PLLA (Sabino, Ronca, & Muller, 2000). It has also shown useful properties as osteosynthesis materials and received the approval of the Food and Drug Administration (FDA) to be used as suture materials in gynecology (Sabino et al., 2000). In spite of the aforementioned benefits, all of above the polyesters are hydrophobic which may lead to complement activation and liver accumulation and they also lack surface cell recognition functions for specific mucoadhesion or receptor recognition (Ciardelli et al., 2005). Not only to improve the mechanical

* Corresponding author. Tel.: +82 63 270 2351; fax: +82 63 270 2348.
E-mail address: Khy@chonbuk.ac.kr (H.Y. Kim).

0144-8617/$ - see front matter © 2009 Elsevier Ltd. All rights reserved.
doi:10.1016/j.carbpol.2009.07.009

properties and weak processibility of biopolymers but also to increase hydrophilicity of synthetic polyesters; polysaccharides have been modified through blending, chemical derivation, and graft copolymerization (Ciardelli et al., 2005; Lindahl & Höök, 1978). Importantly, these copolymers combine the advantage of the hydrophobic polyester for the drug encapsulation, and those of polysaccharide for functional groups onto the surface of nano moiety. Thus by grafting PDO on dextran, its supramolecular structures should be of a substantial importance for the development of blood contacting biomaterials. Specifically, this kind of novel copolymers or its micelles might be more desirable as drug carriers and *in vivo* applications.

Various studies have already been carried out towards the grafting of polyester onto the polysaccharide backbone. For instance, Abdurrahmanoglu and co-worker synthesized dextran-acrylamide gels and observed that swelling degree decreased by increasing the acrylamide monomer concentration due to the formation of more crosslinking points that cause tighter network structure (Abdurrahmanoglu & Firat, 2007). Ciardelli and co-workers studied the bioactivity of PCL blends with different polysaccharides (dextran, gellan, and starch) and found out that starch and gellan are superior to dextran for the production of bioartificial blends (Ciardelli et al., 2005). Wang and co-workers analyzed the microstructure of starch-g-PPDO copolymers with one and two-dimensional NMR spectroscopy (Wang, Yang, Wang, Zhau, & Jin, 2004). He and co-workers observed better thermal stabilities of starch-g-PPDO copolymers with longer side chain than shorter chain length (He et al., 2006). Further, Chen and co-workers synthesized PVA-g-PPDO copolymers and found out that the molecular weight of the copolymers was dependant on the amount of catalyst (stannous octoate) (Chen, Zhou, Wang, Wang, & Yang, 2006). Recently, our group has studied the aqueous dispersion of PCL-grafted dextran (PGD) nanoparticles (Bajgai et al., 2008a; Bajgai, Aryal, Lee, Park, & Kim, 2008b), biocompatibility of PGD scaffolds, and *in vitro* degradation of PGD matrices (Bajgai et al., 2008a, 2008b). Nevertheless, dextran-g-PPDO copolymers have not been reported in the literature.

In this work, we have synthesized poly(1,4-dioxan-2-one) grafted dextran through the grafting between the hydroxyl groups of the dextran and the 1,4-dioxan-2-one (PDO) monomer in the presence of stannous octoate [$Sn(Oct)_2$] catalyst. This paper reports the controlled synthesis of poly(1,4-dioxan-2-one)-grafted dextran copolymers and their efficiency in aqueous dispersion. These results would be promising in the biomedical fields such as, drug delivery and tissue-engineering applications. In addition to biomedical applications, these copolymers will find their uses not only as a compatibilizer for PPDO/dextran blend but also in environmentally friendly materials.

2. Experimental part

2.1. Materials

Dextran (*Leuconostoc mesenteroides*, M_W: 8500–11,500 Da), 1,1,1,3,3,3-hexamethyldisilazane (HMDS) (99.9%), triethylamine (99%), and stannous 2-ethyl hexanoate [$Sn(Oct)_2$] were purchased from Sigma–Aldrich Inc., USA. PDO was provided by Meta Biomedical Co., Korea. All the above chemicals were pure and analytical grade and used as received. $Sn(Oct)_2$, from Aldrich Chemical Co., USA, was used after being dissolved in dry toluene (0.039 M). All the other chemicals used in this research were purchased from Showa Chemical Ltd., Japan.

2.2. Synthesis of dextran-g-PPDO

Graft copolymer was synthesized as reported earlier (Bajgai et al., 2008a, 2008b). Briefly, dextran (1 g: 0.001 mol) was dissolved in dimethyl sulfoxide (10 wt.% dextran) along with the addition of desired quantity of triethylamine and HMDS under nitrogen flow with previously dried syringes. The reaction condition was kept at 60 °C for 50 h. 8 mL of tetrahydrofuran (THF) and 5 mL of toluene were added just after the 4 h of reaction proceeded to make homogenous reaction condition. After the completion of reaction, silylated dextran was precipitated in cold water; vacuum dried, and finally distilled azeotropically in toluene. Protection yields were calculated by ^{1}H NMR (Bajgai et al., 2008a, 2008b). Silylated dextran, with the highest protection yield, has been selected for the ring-opening polymerization of PDO.

Further, ROP of PDO was performed in a previously dried three-necked round bottom flask equipped with a stopcock and a rubber septum, under nitrogen condition. Silylated dextran, which acts as a macro initiator, was subjected for the ROP of PDO in toluene (10 wt.%) in presence of [$Sn(Oct)_2$] catalyst. Polymerization was carried under nitrogen at 100 °C for 48 h. The reaction product was recovered by precipitation in hexafluoroisopropanol/methanol system and dried under vacuum. Finally, silylated graft copolymers were dissolved in THF (10 wt.%, PPDO-grafted silylated dextran) along with the addition of a slight excess of aqueous 0.1 M HCl with respect to the number of $-OSiMe_3$ functions. After 2 h, the deprotected copolymers were recovered by precipitation in heptane and dried under vacuum. We synthesized five different products and the polymers obtained with different feed ratio are referred as PODEX 1, PODEX 2, PODEX 3, PODEX 4, and PODEX 5, as mentioned in Table 1.

2.3. Preparation of PODEX micelles

Core–shell micellar nanoparticles were prepared through the self-assembly of graft copolymers in triple distilled water using co-solvent evaporation technique. About 10 mg of copolymer was dissolved in HFIP (1.0 mL) and dropped into 10 mL of triple distilled water under moderate stirring (150 rpm) at room temperature. The organic phase was allowed to evaporate under reduced pressure until the final volume of the each sample solution was reduced to 10 mL.

2.4. Sample preparation for CMC measurement

Polymeric micellar solutions of various concentrations (0.1–1000 mg/L) were prepared separately by dissolving suitable amount of polymer in triple distilled water as mentioned earlier in this manuscript (Preparation of PODEX micelles). The pyrene solution in acetone (6×10^{-5} M) was added to the de-ionized water to make a pyrene concentration of 1.2×10^{-6} M, and acetone was removed under reduced pressure at 30 °C for 3 h. This solution was mixed with copolymer solutions (0.1–1000 mg/L) resulting a constant pyrene concentration of 6×10^{-7} M. All the solutions were stirred overnight and filtered by 0.2 μm filters before spectrofluorometric measurement.

2.5. Characterization of PODEX

^{1}H NMR and ^{13}C NMR spectra of samples were recorded by JNM-Ex 400 FT-NMR spectrometer (JEOL Ltd., Japan) with 15% (w/v) sample solution in dimethyl sulphoxide-d_6 (DMSO-d_6) and tetramethylsilane (TMS) was used as an internal reference. Fourier-transform infrared (FT-IR) spectra were recorded with KBr pellets using an ABB Bomen MB100 Spectrometer (Bomen Inc., Canada).

The molecular weight and molecular weight distributions for PODEX were measured by gel permeation chromatography (GPC). GPC measurements for PODEX 1–2 were made via Waters 150C (Polymer Laboratories, England) by low angle light scattering

Table 1
Dextran-g-PPDO copolymer synthesized by ROP of PDO with dextran using $(Sn(Oct)_2$ catalyst.

Sample	Molar ratio (PDO/OH)	Cat:OH (mol:mol)	Reaction condition	Molecular weight by GPC		[a]Degree of polymerization of PPDO (DP)	[b]Degree of substitution (DS)	[c]Molecular weight (Mn) by ^{1}H NMR
				M_w	M_n			
PODEX 1	30	500	100 °C, 30 h	94,700	76,100	50	0.38	70,070
PODEX 2	40	500	100 °C, 30 h	100,200	55,600	51	0.28	55,153
PODEX 3	50	500	100 °C, 30 h	115,300	65,500	52	0.32	62,615
PODEX 4	60	500	100 °C, 30 h	111,700	69,200	49	0.36	65,777
PODEX 5	70	500	100 °C, 30 h	117,300	66,000	57	0.31	65,872

[a] The M_n was calculated by 1HNMR as follows: $M_n = 10{,}000 + (DS \times DP \times 31 \times 102)$.
[b] The degree of polymerization of PPDO, calculated by ^{1}H NMR: $DP = I_{\beta,a}/I_{\beta,b}$.
[c] The degree of substitution of PPDO: $DS = I_{\beta,b}/2I_{H1}$.

technique equipped with a refractive index detector, and M_W calibration with polystyrene standard columns using chloroform as a mobile phase at the flow rate of 1.0 mL/min. The copolymers, PODEX 3–5, were soluble only in HFIP. Hence, GPC measurements for PODEX 3–5 were made via Waters 515 (Shodex, USA) with light scattering technique (RI detector). PMMA was used as a calibrant and HFIP as a mobile phase (flow rate: 1 mL/min).

Wide-Angle X-ray Diffraction (WAXD) profiles of these copolymers were measured on a Rigaku D/Max-Ra X-ray diffractometer employing Ni filtered Cu Kα radiation (30 kV, 50 mA, 1.5418 Å). The scanning rate was 0.04°/s.

Thermogravimetric analysis (TGA) was carried on Perkin-Elmer TGA 6 thermogravimetric analyzer (Perkin-Elmer Inc., USA) equipment under a nitrogen atmosphere with a heating rate of 10 °C/min in the range of 25–600 °C. Differential scanning calorimetry (DSC) experiments were carried by a DSC Q100 V 7.3 build 249 (Perkin-Elmer Inc., USA) thermal analysis system. Samples (5 mg) were first heated from −50 to 148 °C with a heating rate of 10 °C/min under nitrogen atmosphere, held for 5 min to remove thermal history, cooled to −50 °C, and finally heated to 148 °C for second heating scan.

2.6. Micelles characterization

Critical micelle concentration (CMC) of the polymeric micelles was determined by a fluorescence method based on solubilization of water-insoluble fluorescent dye (pyrene) into polymer particles in triple distilled water. Excitation spectra (λ_{em} = 390 nm) of pyrene were measured at various polymer concentrations using Hitachi Fluorescence Spectrometer 2514071-05 (Hitachi Co., Japan). CMC value of the polymeric micelle was determined using intensity ratio of band 336–334 nm of pyrene in excitation spectra. Bandwidths used for excitation and emission were 5 and 1.5 nm, respectively. The intensity ratio of I_{336}/I_{334} against polymer concentration (log C) in pyrene excitation spectra was plotted.

Size and surface morphology of the polymeric micelles were observed by AFM nanoscope IV multimode (Digital Instrument, MicroMash Co., USA) in tapping mode using Si cantilever with a spring constant of 305 N/m and a resonance frequency of 75 kHz. Scanning was performed at scan speed of 1.85 Hz. Samples for AFM observations were prepared as a drop-coated film on the argon dried Si (1 1 1) wafers. 10 μL of copolymer solution (1 mg/mL) was dropped on wafers using 100 μL pipette and allowed settle for 30 s. The additional solution was removed by sucking out through pipette tip. Above wafer was allowed to dry at room temperature up to 15 min before AFM observation. Furthermore, morphological examination of the copolymer micelles was performed using a H7650 transmission electron microscope (Bio-TEM, Hitachi Co., Japan). A drop of aqueous PODEX solution (1 mg/mL) was dropped into a 400 mesh copper grid coated with carbon and was stained with phosphotungstic acid. The sample was air dried followed by vacuum dry for 24 h before TEM observation. Average particle size and size distribution were determined by dynamic light scattering method by Particle Size Analyzer (Malvern System 4700 instrument CO., UK) equipped with the aid of vertically polarized light supplied by helium–neon laser (λ = 632.8 nm, Cryonics) and operated with a power of 2 mV at scattering angle of 90° at room temperature. Zeta potential of the micelles was determined by electrophoretic light scattering (ELS) measurement (ELS 8000/6000, Otsuka Electronics Co., Japan) with a measuring angle of 20° when compared to the incident beam. Before analysis, samples were sonicated in an ultrasonicator bath for 1 min.

3. Results and discussion

3.1. Synthesis and characterization of PODEX

Dextran-g-PPDO copolymers were synthesized by a three-step procedure (Scheme 1). First of all, dextran was silylated by HMDS in order to protect number of hydroxyl groups with trimethyl silane (TMS) groups. This silyl group is used to achieve solubility in organic solvent, control the number of reaction sites and obtain longer PPDO chain (Bajgai et al., 2008a, 2008b; Kricheldorf & Damrau, 1998). HMDS is the best choice for controlled silylation of hydroxyl function because of high protection yield and protect degradation of dextran chain (Ouchi et al., 2003). In the first step, silylation reaction was carried out in DMSO as the solubility preference of dextran. After 4 h of reaction, 5 mL of toluene and 8 mL of THF were added to the reaction mixture to maintain the homogenous condition. The silylation reaction was carried out at 60 °C for 50 h. After precipitation in cooled water, the silylated derivative was dried in oven and characterized as 81% protection yield and 2.5° of substitution as described previously (Bajgai et al., 2008a, 2008b). Protection yield percentage and degree of substitution (DS) were calculated by ^{1}H NMR as described earlier using Eq. (1) and (2), respectively (Bajgai et al., 2008a, 2008b; Ouchi et al., 2003).

$$\text{Yeild } \% = \frac{A_{OSiMe_3}}{A_{Glucosidic}} \frac{6 \times 100}{27} \quad (1)$$

$$DS = \frac{3\ (\text{Yeild } \%)}{100} \quad (2)$$

where A_{OSiMe3} and $A_{GlysodicH}$ are the respective areas of trimethyl silyl groups at 0.15 ppm and glycosidic protons centered at 3.2–4.2 ppm. DS is the degree of substitution of silyl groups. The silylation step was preferred to enhance the ROP with longer grafts on the dextran backbone.

In the second step, ROP of PDO has been carried out using remaining hydroxyl groups of protected dextran as a macroinitiator and $Sn(Oct)_2$ as catalyst. Silylated polymer with degree of substitution 2.5 was selected for ROP to obtain larger chain of PPDO graft. Approximately 31 hydroxyl groups are free and 154 groups

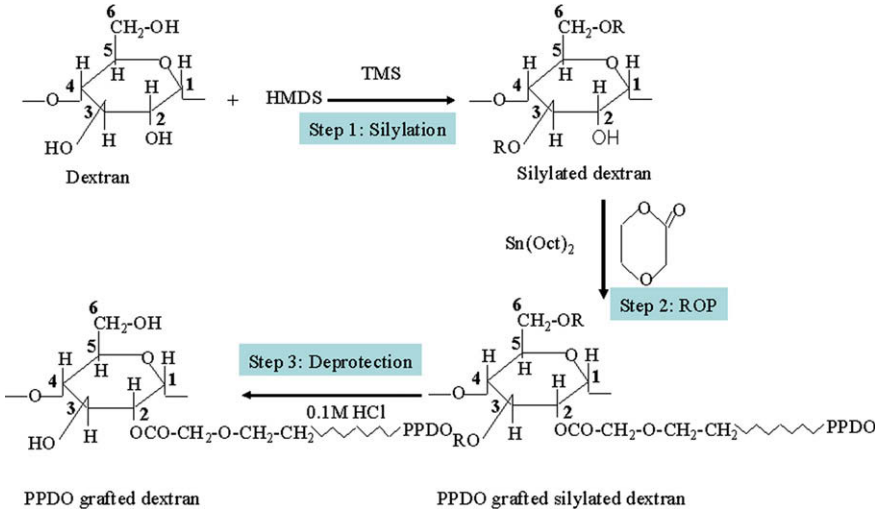

Scheme 1. Synthesis route and structure of PPDO-grafted dextran (dextran-g-PPDO). R represents –$SiMe_3$ (trimethyl silyl) group.

are protected, out of initial 185 hydroxyl groups in 61.7 glucose units of single dextran molecule (M_W, 10,000 Da). The remaining free hydroxyl groups which act as macroinitiators are activated by catalytic amount of $Sn(Oct)_2$ in toluene at 100 °C followed by polymerization with a calculated amount of PDO at 150 °C for 48 h. Finally, silyl groups of copolymers were removed by acid hydrolysis with the addition of slightly excess amount of 0.1 M HCl. The reaction conditions and the results of the dextran-g-PPDO copolymers are summarized in Table 1.

FT-IR spectra of the dextran and PODEX 1 are shown in Fig. 1. FT-IR spectrum of dextran exhibited a broad band at 3398 cm^{-1} (curve A, Fig. 1) due to O–H stretching which is reduced in case of grafted copolymer (curve B, Fig. 1). A band at 2927 cm^{-1} is attributed to CH and CH_2 stretching vibrations. The partially overlapped bands at 1200–800 cm^{-1} and 1270–1000 cm^{-1} are associated with C–O–C and C–O absorptions, respectively. Further, PODEX 1 shows a strong and sharp peak at 1747 cm^{-1} for C=O stretching of ester groups, which is absent in dextran. Also, there is distinct CH_2 rocking band (curve B, Fig. 1) at 720 cm^{-1}, which is further in agreement with PPDO grafts on dextran backbone. Additionally, the sharp peak at 1431 cm^{-1} confirms the absence of monomer in graft copolymer. The absorbance at 1,651 cm^{-1} is due to the H–O–H (hydrogen bonding) group. In addition, the appearance bands for C–H (1460 and 1357 cm^{-1}) and O–H vibrations (1420 cm^{-1}) are in support with CH_2OH group of glucopyranose unit.

Structures of the PODEX copolymers with various PPDO compositions were further analyzed by both proton (^1H) and carbon (^{13}C) NMR spectroscopy as depicted in Fig. 2. The labels of the protons and carbons are assigned in the molecular structure of PODEX 1.

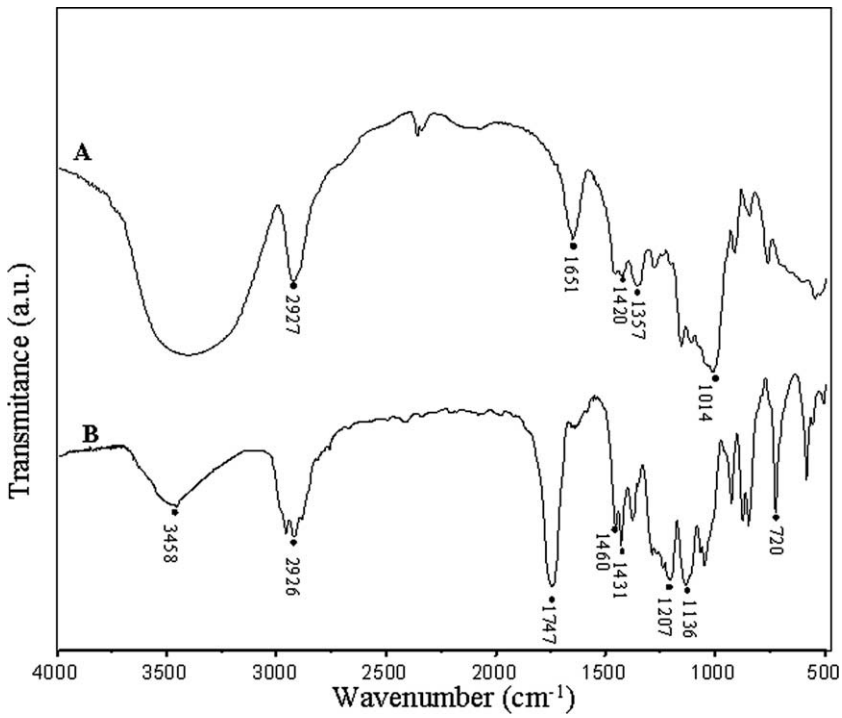

Fig. 1. FT-IR spectra of (A) dextran and (B) PODEX 1, recorded from KBr pellet.

In molecular structure of Fig. 2, numbers 1–6 denote the carbons in the dextran unit, 7 and 8 represent the hydroxyl proton of dextran and terminal hydroxyl proton of PPDO, respectively. Similarly, Greek symbols (α–γ) indicate carbons in the PDO unit. The proton NMR of PODEX 1 gives the peak at 4.16 ($H_{\alpha,a}$, –OCO**CH_2**O–, s, 2H, in chain), 4.15 ($H_{\alpha,b}$, –OCO**CH_2**O–, s, 2H, chain initial), 3.82 ($H_{\beta,a}$, –OCH_2**CH_2**OCO–, t, 2H, in chain), 3.51 ($H_{\beta,b}$, –OCH_2**CH_2**OH, t, 2H chain end), 4.34 ($H_{\gamma,a}$ OCH_2**CH_2**OCO–, t, 2H, in chain), 4.23 ($H_{\gamma,b}$, –OCH_2**CH_2**OH, t, 2H, chain end), and 3.43 ppm (8, s, terminal OH) for PPDO grafts, along with anomeric proton signal at 5.1–5.2 ppm (H_1) and glycosidic proton signals at 3.69 (H_2), 3.27 (H_3), 3.37 (H_4), 3.67 (H_5), 3.68 ($H_{6,a}$), and 3.69 ppm ($H_{6,b}$) of dextran backbone. In the case of ^{13}C NMR, chemical shifts are exhibited as: 61.9 (C_α, OCO**CH_2**), 63.3 (C_β, O**CH_2**CH_2), 60.16 (C_γ, OCH_2**CH_2**), and δ170.3 ppm (carbonyl carbon, **OCO**, not shown in spectra) for PPDO. Also, ^{13}C shifts for dextran backbone are seen in the range of 60.16–68.4 ppm, as mentioned in Fig. 2. As shown in Fig. 2, the carbon and proton NMR spectra of PODEX show the peaks of both dextran and PPDO units, conforming unequivocally the presence dextran along with pendant PPDO chains. The degree of polymerization of PPDO (DP), the degree of substitution (DS), and molecular weight have been calculated by ^{1}H NMR {DP = $I_{\beta a}/I_{\beta b}$, DS = $I_{\beta b}/2I_{H1}$, M_n = 10,000 (DS × DP × 31 × 102)}. It is clearly observed that DP (50–57), DS (0.28–0.38), and M_n (55,153–70,070) varied with the change in molar feed ratio. Similarly, the numbers of grafted PDO units per 100 anhydroglucose units in dextran were calculated following earlier reference (Wang et al., 2004). Units of PDO were increased (280–380) with the increase in M_n value.

Though, M_W of PODEX 1 is lower and in agreement with feed ratio, M_n value is slightly higher in proportion compared to other samples. It might be due to the fact that lower in PDO/OH ratio favors the reaction efficiency (Li, Chen, Cheng, & Wang, 2008a; Li et al., 2008b). This could be ascribed to be very less homopolymer produced during reaction with lower PDO/OH ratio. Hence, M_n values of PODEX 1 are slightly higher in proportion than other samples. It is further supported by lower PDI (M_W/M_n) values in the case of PODEX 1 than other samples.

Molecular weights of the copolymers were determined using GPC. Polymers with lower PPDO content (PODEX 1 and 2) were soluble in $CHCl_3$, whereas the others (PODEX 3, 4, and 5) with higher PPDO concentrations were soluble in HFIP. Molar feed ratio (PDO/OH) and the results of the polymerization have been summarized in Table 1. The molecular weight of the graft copolymers increased (M_W: 94,700–117,300) with increasing the PDO/OH (dextran) feed ratio (30–70). All the polymers showed the relatively wide molecular distribution and polydispersity (M_W/M_n) from 1.24 to 1.8. This fact might be due to intermolecular ester interchange at high temperature, till the establishment of most probable molecular mass distribution.

Thermal transition temperatures of various PODEX copolymers with same dextran backbone were analyzed through DSC and the results are summarized in Table 2. Glass transition (T_g) and crystalline temperatures (T_c) were observed at the range of −17 to −29 °C and 20–28 °C, respectively (spectra not shown). Such variation in T_g and T_c is not only due to difference in the molecular weights of the grafted PPDO unit but also variation in DS and DP among copolymers. We can find that the T_g of PODEX 3 (−17 °C) is higher than that of PODEX 1 (−28 °C). Same trend is observed for crystallization and melting temperatures. Also, the T_g for pure PPDO (Viscosity average molecular weight, 1.88×10^5 gmol^{-1}) is −9.5 °C as reported in earlier literature (Zhou et al., 2006), which is in agreement with our obtained results for PODEX copolymers (PODEX 1–3). Also, PODEX 1, 2, and 3 exhibited single melting endotherms at 82, 93, and 100 °C, respectively (Table 2). Since dextran moiety in PODEX is amorphous and does not produce melting temperature, this result represents the melting temperatures of semicrystalline PPDO units. The melting temperature was increased with the increment in PDO fraction in the PODEX copolymers. It seems that the crystal structure of dextran-g-PPDO is less perfect than that of the PPDO homopolymer (Zhou et al., 2006), as indicated by the lower melting point due to the presence of more defect sites in the crystalline phase originating from the short length of the grafted PPDO. Nevertheless, it is believed that crystallization rate depends on two factors, nucleation and crystal growth rate. Hence,

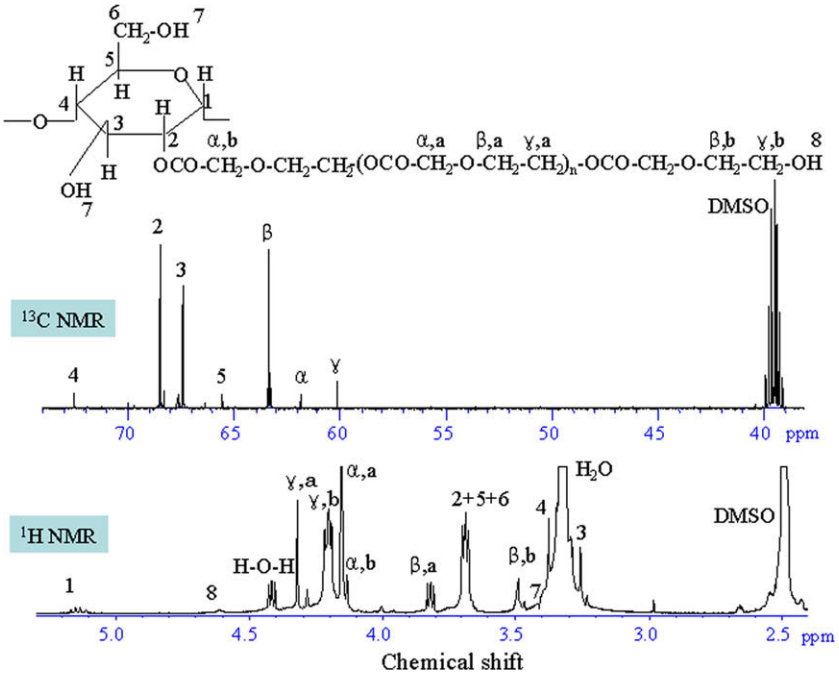

Fig. 2. ^{1}H and ^{13}C NMR recorded at 15% solution of PODEX 1 copolymer in DMSO-d6 in presence of TMS as an internal reference.

Table 2
Thermal properties of PODEX graft copolymers derived from TGA and DSC analysis.

Samples	Second run DSC data of the copolymers (° C)			ΔH_c (J/g)	ΔH_m (J/g)	X_c (%)	TGA (°C)	
	T_g	T_c	T_m				T_{onset} (°C)	T_d (°C)
PODEX 1	−28	25	82	−23	45	32	195	301
PODEX 2	−29	20	93	−28	56	40	251	276
PODEX 3	−17	28	100	−30	57	40	276	301

T_g, T_c, T_m, and T_d are the glass transition, crystallization, melting, and degradation temperatures, respectively.

it can be inferred that the single T_g, T_m, and T_c obtained for the copolymers represents the complete miscibility of all the segments in the copolymers.

The percentage crystallinity (X_c%) of the PODEX graft copolymer decreased from 40% (PODEX 3) to 32% (PODEX 1) as shown in Table 2. This crystallinity was calculated by Eq. (3) (Jiang, Azim, & Gross, 2007; Kazunori, Harada, & Nagasaki, 2001; Li et al., 2008a, 2008b; Ye, Zhang, Jia, He, & Ge, 2002).

$$X_c\% = (\Delta H_f / \Delta H_f^0) \times 100 \quad (3)$$

where ΔH_f = heat of fusion, ΔH_f^0 = heat of fusion for 100% crystalline PODEX (considered as 141.18 J/g).

The degradation temperatures of the polymers are summarized in Table 2. The initial to maximum weight loss ranges are 195–301, 251–276, and 295–301 °C for PODEX1, PODEX 2, and PODEX 3, respectively. We observed single stage decomposition behavior of the copolymers (Table 2, Figures not shown). It is revealed that the increase amount of PPDO content increases the thermal stability of the copolymer. The variation in the degradation phenomena is due to the fact that different copolymers have different amount of PPDO as their side chain.

X-ray diffraction patterns of PODEX copolymers (Figures not shown) displayed their main peaks at 2θ (degree) equal to 21.9, 23.8, and 29.3°, which are those typical of an orthorhombic crystalline unit cell and attributed to the PPDO units (Xu et al.,1998; Zhou et al., 2006). The relative peak intensity of the samples was similar for all copolymers and it is evidencing a similar crystalline degree for all graft copolymers. Also it is clear that PPDO segments retain their crystal structure and intensity has been increased with increasing content of PPDO graft unit. These results were also supported by DSC results.

3.2. Determination of CMC

We have selected co-solvent evaporation technique (acetonitrile/water or HFIP/water system depending upon the solubility of the polymer) for the self-assembly of amphiphilic graft copolymers. Also the organic solvent of this system can be easily removed at room temperature. The micelle core made up of PPDO can serve as a microenvironment for the incorporation of lipophilic moieties; while the corona shell, composed of dextran backbone, serves as a stabilizing layer between the hydrophobic core and the external aqueous environment (Chen, Chen, Hu, & Wang, 2005; Chen et al., 2006). Also, Location of hydrophobic segment at this stage is well characterized by fluorescence spectra using pyrene as a fluorescence probe. Pyrene was selected as probe to investigate the self-aggregation behavior of the copolymer in an aqueous environment. When exposed to a polymeric micelle aqueous solution, pyrene molecules preferably participate in the hydrophobic microdomains of the micelles rather than the aqueous phase. Fig. 3 shows the typical fluorescence spectra of pyrene in aqueous medium. At low concentrations, there were low or negligible changes in

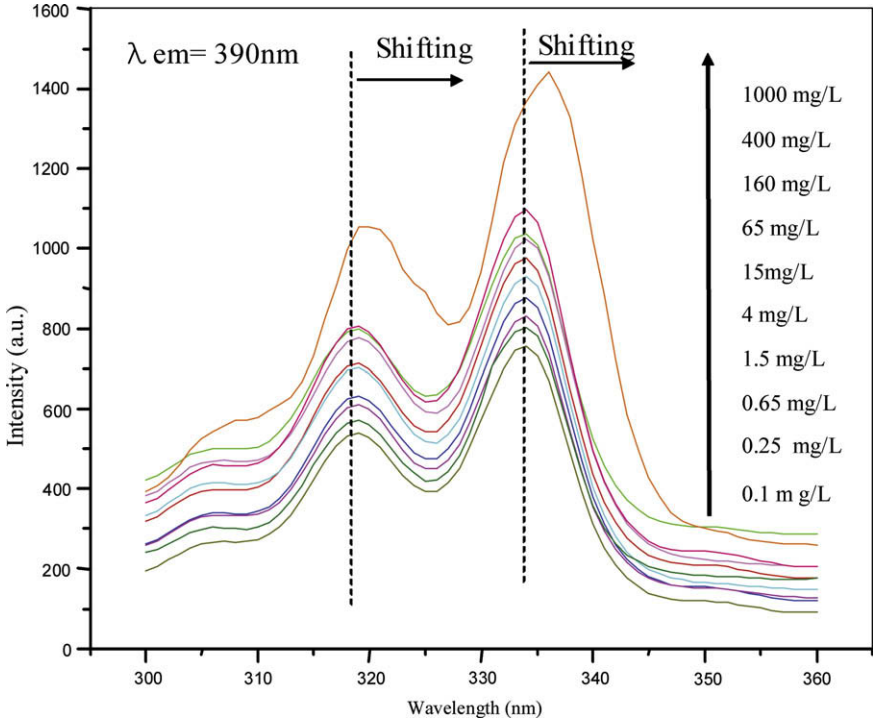

Fig. 3. Excitation spectra of pyrene for PODEX 1, as a function of copolymer concentration.

Table 3
Characterization of dextran-g-PPDO nanoparticles. All values are expressed as mean ± SD (n = 4).

Samples	Particle size (nm)			ζ-potential (mV)	CMC (mg/L)
	AFM	TEM	DLS		
PODEX 1	15 ± 0.9	13 ± 1.3	71 ± 3.3	−14 ± 0.2	3.1 ± 0.02
PODEX 2	27 ± 1.1	22 ± 1.0	77 ± 2.7	−18 ± 0.3	2.9 ± 0.04
PODEX 3	38 ± 0.3	41 ± 0.5	79 ± 2.6	−27 ± 0.2	1.3 ± 0.03
PODEX 4	58 ± 0.5	59 ± 0.8	85 ± 4.3	−28 ± 0.1	1.09 ± 0.01

CMC represents the critical micelle concentration, obtained by pyrene excitation spectra at constant emission of 390 nm.

fluorescence intensity and a shift of (0, 0) band at 334 nm. As the concentration of the micelles increased, a remarkable increase of the total fluorescence intensity and a red shift of the (0, 0) band from 334 to 336 nm were observed. On the basis of intensity ratio, the CMC values of the polymers were calculated by the cross over points at low concentration ranges (Bajgai et al., 2008a, 2008b). The CMC values were obtained in the range of 3.2–1.09 mg/L as mentioned in Table 3. Copolymers with longer PDO blocks had higher the CMC value, similar to graft copolymers (Xie, Han, Wang, He, & Zhang, 2008). The graft copolymer having a higher surface area provides more rigid or compact hydrophobic core in self-aggregates.

3.3. Morphology of dextran-g-PPDO micelles

Morphology and size of the polymeric micelles were analyzed by AFM (Fig. 4A–D), BioTEM (Fig. 4E–H), and DLS measurement and observations are summarized in Table 3. Both AFM and TEM are the microscopic tools for the analysis of size and morphology of the nanoparticles and micelles that are adsorbed on substrate surface. Specifically, AFM is a facile technique that can probe the nano species for producing high-resolution 3-D topographic images without sample staining. DLS is mainly used for the measurement of average hydrodynamic diameter in colloid state.

AFM observations revealed that most of the particles from all the samples were discrete smooth and regular with 15 to 58 nm diameters (Table 3, Fig. 4A–D). Such morphology has been confirmed by TEM images (Fig. 4E–H). The core size of the micelles is in the range of 13–59 nm as observed in TEM images (Table 3). Both AFM and TEM observations exhibited linear increment in core size of the particle with increasing the content of PPDO. Nevertheless, size measured by AFM is observed larger than that of TEM. It is known that TEM has high-resolution (0.1 nm) and can give more accurate size than AFM. In the case of AFM, its tip is not capable of distinguishing the neighboring nanoparticles at distances less than its radius. Hence, AFM images might have included some aggregates and showing some particles larger in size than the images observed under TEM (Zeng, Koshizaki, & Sasaki, 1999).

DLS measurement showed a unimodal size distribution with a mean hydrodynamic diameter in the range of 71–85 nm. The difference in micelles size as measured by AFM, TEM and DLS was attributed that the latter is the hydrodynamic diameter of micelles in solvated state, instead the former two (AFM, TEM) reveal the morphological size in solid and dry state (Xie et al., 2008; Xu et al., 1998). It is assumed that PPDO moieties would be tightly held in the micelle core, with the dextran blocks loosely packed around it. Hence, the overall diameter obtained by DLS represented the core dimension and the shell thickness (Xie et al., 2008).

Similarly, the negative zeta potential (−14 to −28) of the micelles increased with increase in PPDO quantity in the copolymer (Table 3). Such gain in negative zeta potential among the copolymers might be due to the increase in the number of ionisable carboxylic groups with the increase of PPDO quantity (Lindahl & Höök, 1978). Furthermore, the stability of the particles was observed by incubating particles at 37 ± 1 °C in PBS at physiological condition for 1 month. This stability study of the particles prepared in PBS reveals that particles are promising in delivery systems.

4. Conclusions

Ring-opening polymerization of 1,4-dioxan-2-one on dextran backbone obtained novel graft copolymers, dextran-g-PPDO, with various graft structures. Increase in the PDO content induced the increase in thermal properties of the graft copolymer. Similarly, varying the amount of PPDO unit in the polymer can control CMC and micelle size. Also the micelle like nanoparticles showed the core shell geometry having average diameter 30–58 nm, as measured by AFM. The CMC of the micelles was investigated in the range 3.2–1.09 mg/L in triple distilled water. PODEX micells would be a promising vehicle for the delivery of hydrophobic drugs. Though all the batches of PODEX may carry hydrophobic drug, it is desirable to perform *in vitro* drug delivery experiment and to choose the best drug carrier.

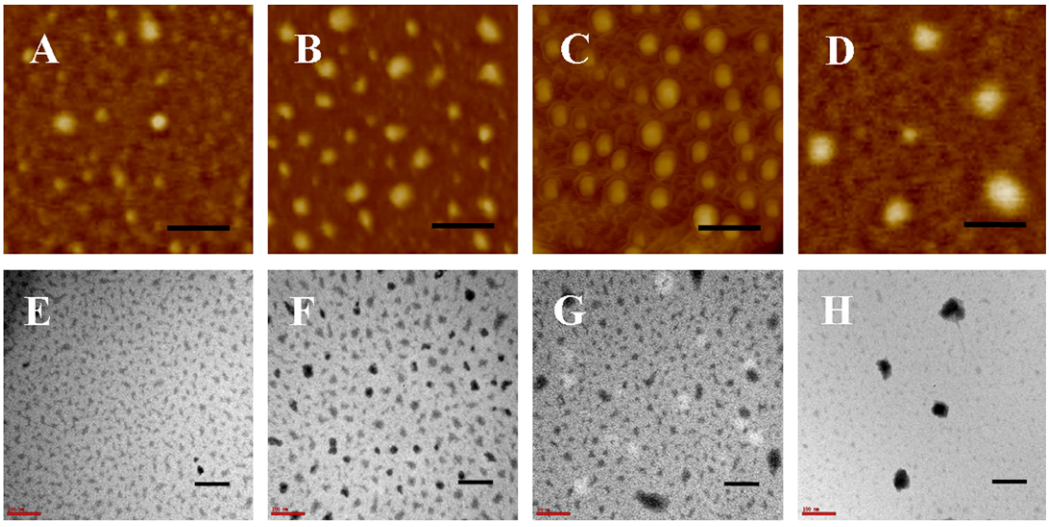

Fig. 4. AFM (A–D) and BioTEM (E–G) images of PODEX 1 (A and D), PODEX 2 (B and F), PODEX 3 (C and G), and PODEX (D and H) nanoparticles. Scale bar is 100 nm for all the images.

Acknowledgements

This research was supported by the Korea Research Foundation (KRF2007-211-D00032, Korean Government Project N0: 10028211), the Ministry of Commerce, Industry and Energy Department, and the Regional Research Centers Program of the Korean Ministry of Educational and Human Resources Development through the Center for Healthcare Technology Development, Chonbuk National University, Jeonju 562-756, and Republic of Korea. Authors thank the Korean Basic Science Institute (KBSI), Jeonju, for assistance with AFM measurements.

References

Abdurrahmanoglu, S., & Firat, Y. (2007). Synthesis and characterization of new dextran-acrylamide gels. *Journal of Applied Polymer Science, 106*, 3565–3570.

Anderson, J. M., & Shie, M. S. (1997). Biodegradation and biocompatibility of PLA and PLGA microspheres. *Advanced Drug Delivery Reviews, 28*, 5–14.

Bajgai, M. P., Aryal, S., Bhattarai, S. R., KC, R. B., Kim, K. W., & Kim, H. Y. (2008a). Poly (ε-caprolactone) grafted dextran biodegradable electrospun matrix: A novel scaffold for tissueengineering. *Journal of Applied Polymer science, 108*, 1447–1454.

Bajgai, M. P., Aryal, S., Lee, D. R., Park, S. J., & Kim, H. Y. (2008b). Physicochemical characterization of self-assembled poly (ε-caprolactone) grafted dextran nanoparticles. *Colloid and Polymer Science, 286*, 517–524.

Bhattarai, S. R., Bhattarai, N., Viswanathamurthi, P., Kim, H. Y., Hwang, P. H., & Kim, Y. (2006). Hydrophilic nanofibrous structure of polylactide; fabrication and cell affinity. *Journal of Biomedical Material Research, 78A*, 247–257.

Chen, H., Chen, T., Hu, J., & Wang, C. (2005). Nano aggregates of biodegradable amphiphilic poly(hydroxyethyl aspartamide-co-propyl aspartamide) grafted with poly(D, L-lactide). *Colloids and Surfaces A: Physicochemical and Engineering Aspects, 268*, 24–29.

Chen, J., Jo, S., & Park, K. (1995). Polysaccharide hydrogels for protein drug delivery. *Carbohydrate Polymers, 28*, 69–76.

Chen, S. C., Zhou, Z. X., Wang, Y. Z., Wang, X. L., & Yang, K. K. (2006). A novel biodegradable poly(*p*-dioxanone)-grafted poly(vinyl alcohol) copolymer with a controllable in vitro degradation. *Polymer, 47*, 32–36.

Choi, E. J., Kim, C. H., & Park, J. K. (1999). Synthesis and characterization of starch-*g*-polycaprolactone copolymer. *Macromolecules, 32*, 7402–7408.

Ciardelli, G., Vozzi, V. G., Pracella, M., Ahluwalia, A., Barbani, N., Cristallini, C., et al. (2005). Blends of poly (ε-caprolactone) and polysaccharides in tissue engineering applications. *Biomacromolecules, 6*, 1961–1976.

He, R., Wang, X. L., Wang, Y. Z., Yang, K. K., Zeng, J. B., & Ding, S. D. (2006). A study on grafting poly(1,4-dioxan-2-one) onto starch via 2,4-tolylene diisocyanate. *Carbohydrate Polymers, 65*, 28–34.

Jiang, Z., Azim, H., & Gross, R. A. (2007). Lipase-catalyzed copolymerization of ω-pentadecalactone with *p*-dioxanone and characterization of thermal and crystalline properties. *Biomacromolecule, 8*, 2262–2269.

Kazunori, K., Harada, A., & Nagasaki, Y. (2001). Block copolymer micelles for drug delivery: Design, characterization and biological significance. *Advanced Drug Delivery Reviews, 47*, 113.

KC, R. B., Aryal, S., Bhattarai, S. R., Khil, M. S., & Kim, H. Y. (2007). Amphiphilic triblock copolymer based on poly(*p*-dioxanone) and poly(ethylene glycol): Synthesis, characterization, and aqueous dispersion. *Journal of Applied Polymer science, 103*, 2695–2702.

Kim, C. H., Khil, M. S., Kim, H. Y., Lee, H. U., & Jahng, K. Y. (2006). An improved hydrophilicity via electrospinning for enhanced cell attachment and proliferation. *Journal of Biomedical Material Research, 78B*, 283–290.

Kricheldorf, H. R., & Damrau, D. (1998). Zn L-lactate-catalyzed polymerizations of 1,4-dioxan-2-one. *Macromolecuar Chemical Physics, 199*, 108.

Li, Y. D., Chen, S. C., Cheng, J. B., & Wang, Z. Y. (2008a). Novel biodegradable poly(1,4-dioxan-2-one) grafted soy protein copolymer: Synthesis and characterization. *Industrial and Engineering Chemistry Research, 47*, 4233.

Li, B., Chen, S. C., Qiu, Z. C., Yang, K. K., Tang, S. P., Yu, W. J., et al. (2008b). Synthesis of poly (lactic acid-b-*p*-dioxanone) block copolymers from ring opening polymerization of *p*-dioxanone by poly(L-lactic acid) macro initiators. *Polymer Bulletein, 61*, 139–146.

Lindahl, U., & Höök, M. (1978). Glycosaminoglycans and their binding to biological macromolecules. *Annual Review of Biochemistry, 47*, 385–417.

Nishida, H., Konno, M., Ikeda, A., & Tokiwa, Y. (2000). Microbial degradation of poly(*p*-dioxanone) isolation of degrading microorganisms and microbial decomposition in pure culture. *Polymer Degradation and Stability, 68*, 205–217.

Ouchi, T., Kontani, T., & Ohya, Y. (2003). Modification of polylactide upon physical properties by solution cast blends from polylactide and polylactide-grafted dextran. *Polymer, 44*, 3927–3933.

Pachence, J. M., & Kohn, J. (2000). *Bioresorbable polymers for tissue engineering. Principles of Tissue Engineering*. San Diego: Academic Press. pp. 267–270.

Sabatie, J., Choplin, L., Doublier, J., Arul, J., Paul, F., & Monsan, P. (1988). Rheology of native dextran in relation to their primary structure. *Carbohydrate Polymers, 9*, 287–299.

Sabino, M. A., Ronca, G., & Muller, A. J. (2000). Heterogeneous nucleation and self nucleation of poly (*p*-dioxanone). *Journal of Materials Science, 35*, 5071–5084.

Wang, X. L., Yang, K. K., Wang, Y. Z., Zhau, Z. X., & Jin, Y. D. (2004). Synthesis and nuclear magnetic resonance analysis of starch-*g*-poly(1,4-dioxan-2-one) copolymers. *Journal of Polymer Science Part A: Polymer Chemistry, 42*, 3417–3422.

Xie, M., Han, H., Wang, W., He, X., & Zhang, Y. (2008). Synthesis and self-assembly of functionalized cyclooctene block copolymers via ROMP micromole. *Chemical Physics, 209*, 544–550.

Xu, Z., Feng, L., Ji, J., Cheng, S., Cheng, Y., & Yi, C. (1998). The micellisation of amphiphilic graft copolymer PMMA-g-PEO in toluene. *European Polymer Journal, 34*, 1499–1504.

Ye, Q., Zhang, Z., Jia, H., He, W., & Ge, X. (2002). Formation of monodisperse polyacrylamide particles by radiation-induced dispersion polymerization: Particle size and size distribution. *Journal of Colloid and Interface Science, 25*, 3279–3284.

Young, Y., Min, B. M., Lee, S. J., Lee, T. S., & Park, W. H. (2005). In vitro degradation behavior of electrospun polyglycolide, polylactide, and poly(lactide-*co*-glycolide). *Journal of Applied Polymer Science, 95*, 193–200.

Zeng, X., Koshizaki, N., & Sasaki, T. (1999). A direct comparison of sizes characterized by TEM and AFM for Fe_2O_3 nanoparticles prepared by laser ablation. *Applied Physics A., 69*(Suppl.), 253–255.

Zhou, Z. X., Wang, X. L., Wang, Y. Z., Yang, K. K., Chen, S. C., Wu, G., et al. (2006). Thermal properties and non-isothermal crystallization behavior of biodegradable poly(*p*-dioxanone)/poly(vinyl alcohol) blends. *Polymer International, 55*, 383–390.